Energy & Environmental Science

COMMUNICATION

View Article Online
View Journal | View Issue

Cite this: *Energy Environ. Sci.*, 2016, **9**, 917

Received 14th December 2015,
Accepted 16th February 2016

DOI: 10.1039/c5ee03764f

www.rsc.org/ees

A redox flow lithium battery based on the redox targeting reactions between $LiFePO_4$ and iodide†

Qizhao Huang, Jing Yang, Chee Boon Ng, Chuankun Jia and Qing Wang*

In the search for a reliable and low-cost energy storage system, a lithium-iodide redox flow lithium battery is proposed, which consists of a lithium anode and an iodide catholyte with $LiFePO_4$ as a solid energy storage material. This system demonstrates a good cycling performance and capacity retention. It can potentially achieve an energy density of 670 W h L^{-1}.

Electrochemical energy storage (EES) is expected to play a pivotal role for smart grid[1] and automotive applications,[2–4] where megawatt-size stationary battery systems and those for extended-range electric vehicles are already commercially available. The lithium-ion battery, as the state-of-the-art EES technology, has been a promising candidate for energy storage systems apart from safety concerns such as thermal runaway.[5] Several redox flow battery concepts including those using lithium as the anode had been reported to address the issues by decoupling the energy storage and power generation.[6–10] Among the various redox flow technologies, the recently reported redox flow lithium battery (RFLB) has the advantages of superior energy density, good scalability and operation flexibility, as well as excellent safety over other technologies.[11,12]

As the half-cell illustrated in Fig. 1, the RFLB exploits the basic structure of a redox flow battery and extracts energy from the lithium-ion battery materials with the assistance of redox shuttle molecules. At the inception of the concept, two redox molecules were employed to pair with each battery material for reversible "redox-targeting" reactions: one redox molecule with a high formal potential that can chemically oxidize the solid active material for effective delithiation, and the other redox molecule with a lower formal potential that can chemically reduce the solid active material for effective lithiation. Hence, by employing solid materials with dense Li^+ storage in the tank, with relatively low concentration redox molecules mediating the reactions in the electrolyte, the RFLB provides an elegant means for achieving high energy density redox flow batteries. As such, the gravimetric and volumetric energy density of the RFLB will largely be determined by the active materials filled in the tanks. In RFLBs, as the molar concentration of the redox molecules is generally lower than the solid active materials, these redox molecules undergo multiple cycles of redox reactions upon operation. For instance, in the previously reported RFLB half-cell[11] where $LiFePO_4$ was used as the cathodic energy storage material with 20 mM ferrocene and its derivatives dissolved in the electrolyte as the redox mediators, for one charging/discharging cycle each molecule will on average experience 10-fold[3] redox-targeting reactions with an equal volume of $LiFePO_4$ to fully exploit its capacity, since the concentration of Li^+ in the material is 3 orders of magnitude higher. Such a high turnover time demands robust redox molecules to ensure a good cycling performance of the RFLB.

Iodide is known to exhibit two redox reactions (I^-/I_3^- and I_3^-/I_2) in various solvents and show excellent chemical reversibility as attested in dye-sensitised solar cells.[13] As the potentials of the two redox couples just straddle the delithiation/lithiation potential of $LiFePO_4$, a single redox species I^- would suffice for both charging and discharging of $LiFePO_4$. As such, the system is expected to be less vulnerable to degradation compared with the case involving

Broader context

More and more countries aim to replace fossil fuel by renewable and environmentally sustainable energy sources in the face of the dire consequences of global warming and depleting hydrocarbon fuel. Both solar and wind power are the most abundant and readily accessible renewable sources. However, the intermittent nature of these two renewable sources would destabilize the grid without appropriate energy storage systems. Electrochemical energy storage systems, compared to other energy storage systems, have the advantages of minimal geographical restrictions, modular design, high efficiency and quick response. Among various electrochemical energy storage systems, redox flow batteries are the most suitable for large-scale energy storage applications. Low energy density, however, remains a challenge for redox flow batteries.

Department of Materials Science and Engineering, NanoCore, National University of Singapore, 117576, Singapore. E-mail: qing.wang@nus.edu.sg

† Electronic supplementary information (ESI) available. See DOI: 10.1039/c5ee03764f

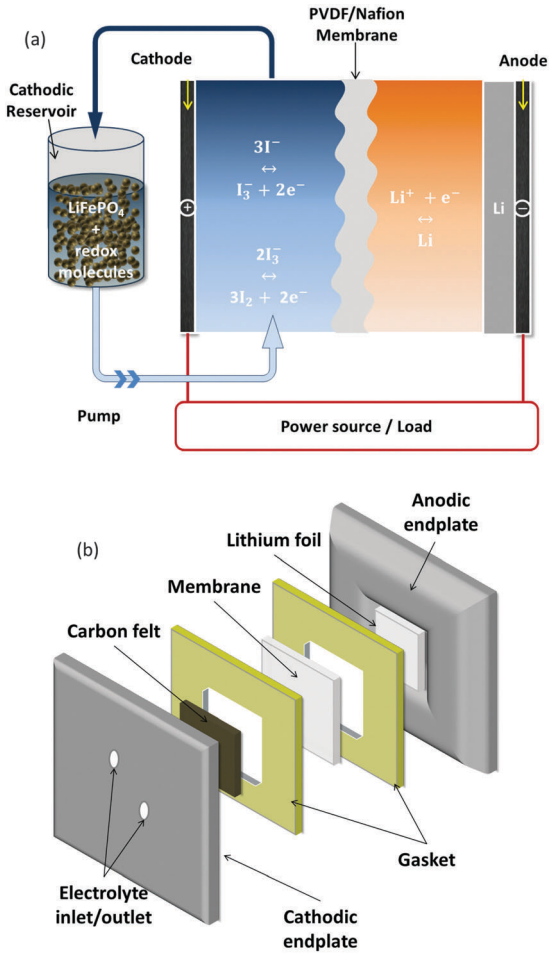

Fig. 1 (a) Schematic of Li-I RFLB and (b) exploded view of the cell structure.

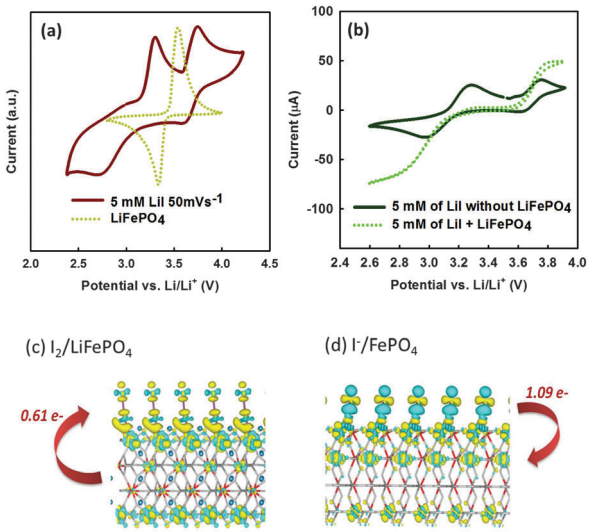

Fig. 2 (a) CV of redox shuttle molecule LiI, as well as the cathodic Li^+-storage material $LiFePO_4$. The electrolyte is 1 M LiTFSI in TEGDME. The scan rate of the CV of LiI is 50 mV s^{-1}. (b) CV of LiI in the absence/presence of $LiFePO_4$. The working electrode is FTO-Al_2O_3-$LiFePO_4$ and the counter and reference electrodes are lithium foils. The electrolyte is 1 M LiTFSI in TEGDME. The scan rate of the CV of LiI is 10 mV s^{-1}. Electron density difference maps for (c) I_2/$LiFePO_4$ and (d) I^-/$FePO_4$ systems. Blue and yellow zones correspond to electron density deduction and enhancement regions, respectively. The charge transfer quantified by the Bader charger analysis is listed for each system.

multiple redox molecules. Hence, here we report a novel RFLB half-cell based on the redox-targeting reactions between iodide and $LiFePO_4$. Meanwhile, as the active material $LiFePO_4$ can achieve 22.8 M of Li^+ storage, the Li-I RFLB cell is anticipated to present a superior cycling performance as well as high energy density.

As reported in many other solvents, LiI undergoes two-electron redox reactions in 1 M lithium bis(trifluoromethane) sulfonimide (LiTFSI)/tetraethyleneglycol dimethylether (TEGDME). The I^-/I_3^- reaction occurs at ~3.15 V (*vs.* Li/Li^+) and the I_3^-/I_2 reaction at ~3.70 V (*vs.* Li/Li^+) as shown in the cyclic voltammetry (CV) measurements in Fig. 2a. The redox potential of $LiFePO_4$ (~3.45 V *vs.* Li/Li^+) sits right in between the potentials of I^-/I_3^- and I_3^-/I_2. Therefore, it is energetically favorable for $FePO_4$ to be chemically reduced by I^- and for $LiFePO_4$ to be chemically oxidized by I_2. The former was reported by Kuss *et al.*[14] The CV of LiI in the presence of $LiFePO_4$ provides further insight into the reactions between the iodide species and the material. As shown in Fig. 2b, a working electrode was prepared by screen printing a layer of Al_2O_3 (~3 μm thick) on a platinized fluorine-doped tin oxide (FTO) glass followed by a layer of $LiFePO_4$ (~100 μm thick). The Al_2O_3 layer acts as a porous spacer that insulates the $LiFePO_4$ layer from FTO but allows for the diffusion of redox molecules in the electrolyte.[15]

In the presence of $LiFePO_4$, two well-defined current plateaus for the oxidation and reduction processes could be observed. The appearance of the catalytic waves indicates that the redox couple was recycled by charge injection in the battery material: I_3^- is regenerated from I_2 by hole injection into the $LiFePO_4$ layer and I_3^- from I^- by electron injection into the $FePO_4$ layer during charging and discharging, respectively. As a consequence, the current is not limited by the diffusion of the redox species and is higher than that obtained in the absence of $LiFePO_4$.[15,16] These steady state currents suggest that $LiFePO_4$ can be oxidized by I_2 and $FePO_4$ can be reduced by I^-.[16]

DFT calculations were carried out to understand the charge transfer processes of the above redox-targeting reactions associated with $LiFePO_4$/$FePO_4$. The computational details can be referred to in the ESI.† Fig. 2c and d show the electron density difference maps of the I_2/$LiFePO_4$ and I^-/$FePO_4$ systems, where the blue and yellow zones correspond to the electron density deduction and enhancement regions, respectively. Upon the interaction of I_2 with $LiFePO_4$, electrons are redistributed so that they flow from $LiFePO_4$ to I_2. The charge transfer is quantified by Bader charge analysis to be 0.61 e^-. As shown in Fig. 2c, the Fe^{2+} in $LiFePO_4$ serves as the dominant redox center, which is oxidized to Fe^{3+} during delithiation. The lithiation of $FePO_4$ is triggered by the interaction with I^-. As shown in Fig. 2d, the $FePO_4$ receives 1.09 e^- from I^- upon interaction and the Fe^{3+} in $FePO_4$ serves as the dominant redox center that is reduced back to Fe^{2+} during lithiation.

The above computational study is corroborated by the chemical lithiation of $FePO_4$ and the delithiation of $LiFePO_4$ with the respective redox species. *Ex situ* X-ray diffraction (XRD)

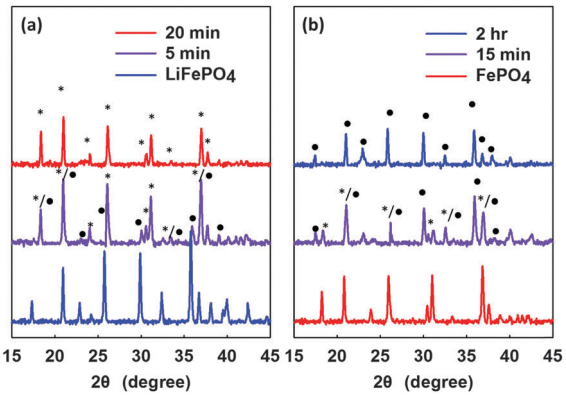

Fig. 3 XRD patterns of $LiFePO_4/FePO_4$ at different time intervals of chemical (a) delithiation and (b) lithiation. * represents the peaks of $FePO_4$ and ● represents the peaks of $LiFePO_4$.

was conducted to monitor the structural changes of $LiFePO_4/FePO_4$ during the chemical delithiation/lithiation processes. In the presence of 20 mM I_2 (~5 times in excess of $LiFePO_4$), $LiFePO_4$ undergoes delithiation and becomes $FePO_4$ in 20 minutes. In the 5 minute interval, the coexistence of the two phases ($LiFePO_4$ and $FePO_4$)[17] was observed, as shown in Fig. 3a. The lithiation of $FePO_4$ by 20 mM LiI is shown in Fig. 3b, which is evidently much slower compared with the delithiation process. In the 15 minute interval, the coexistence of the two phases ($FePO_4$ and $LiFePO_4$) was also identified. The single-phase samples at the end of the reaction unambiguously substantiate that the delithiation of $LiFePO_4$ was complete in 20 minutes, while the lithiation of $FePO_4$ in 2 hours. Their XRD patterns are identical to the pristine samples, proving that both lithiation by I^- and delithiation by I_2 are reversibly completed.

To assess the viability of iodide as a single redox species for battery application, a Li-I RFLB (Fig. 1) half-cell consisting of a cathodic compartment and an anodic compartment separated by a Li^+-conducting polymeric membrane was constructed. In the anodic compartment, the lithium foil is secured on a stainless steel plate. $LiFePO_4$, the active material in granular form, remains in the cathodic reservoir throughout the reactions. And the cathodic electrolyte (LiI dissolved in 1 M LiTFSI/TEGDME) is circulated between the cathodic reservoir and the cathodic compartment by a peristaltic pump. In the cathodic reservoir, the charging process is described by eqn (1) and (2); and the discharging process is described by eqn (3) and (4).

The electrochemical process on the electrode when charging:

$$2I_3^- - 2e^- \rightarrow 3I_2 \quad (1)$$

Chemical delithiation in the reservoir:

$$3I_2 + 2LiFePO_4 \rightarrow 2I_3^- + 2FePO_4 + 2Li^+ \quad (2)$$

The electrochemical process on the electrode when discharging:

$$I_3^- \rightarrow 3I^- - 2e^- \quad (3)$$

Chemical lithiation in the reservoir:

$$3I^- + 2FePO_4 + 2Li^+ \rightarrow I_3^- + 2LiFePO_4 \quad (4)$$

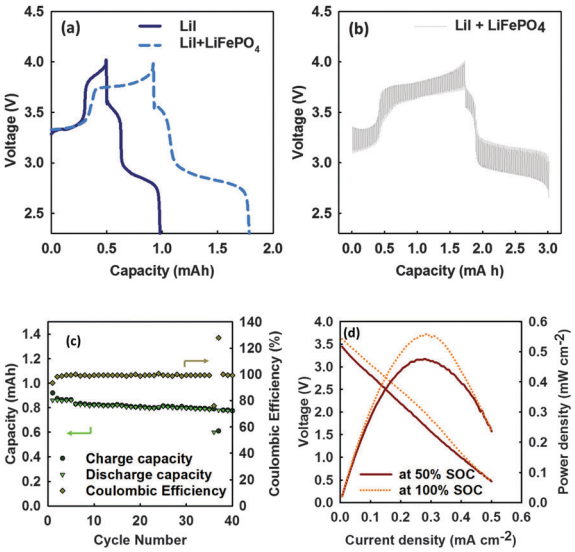

Fig. 4 Charge/discharge performance of a Li-I RFLB cell containing (a) 10 mM LiI with/without 6.4 mg $LiFePO_4$ (20 mM equivalent concentration) loaded in the cathodic reservoir in 2 ml catholyte. (b) GITT measurement of 10 mM LiI with 25 mg $LiFePO_4$. The current density was 0.025 mA cm^{-2} for all three measurements. (c) Capacity retention and CE of the Li-I RFLB cell cycled at 0.075 mA cm^{-2}. (d) Polarization curves at 50% and 100% state-of-charge (SOC) of the Li-I RFLB cell. The current density was gradually increased from 0 to 0.5 mA cm^{-2} for 400 s. In the cell 6.4 mg $LiFePO_4$ was loaded in the cathodic reservoir, circulated with 5 ml of 10 mM LiI in 1 M LiTFSI/TEGDME catholyte.

Total cell reaction:

$$2FePO_4 + 2Li^+ + 2I^- \leftrightarrow 2LiFePO_4 + I_2 \quad (5)$$

Fig. 4 shows the chronopotentiometric measurements of the cell, which clearly indicate that $LiFePO_4$ can be reversibly charged and discharged by I_2 and I^- in the catholyte. With LiI alone (Fig. 4a), two charge (~3.30 V and 3.80 V) and two discharge (~2.90 V and 3.50 V) plateaus can be observed. The lower plateaus correspond to the redox reaction of I^-/I_3^- and theoretically it should be twice as long as that of I_3^-/I_2. Limited capacity of the Li-I RFLB was observed in the absence of $LiFePO_4$ in the cathodic reservoir. In contrast, once $LiFePO_4$ granules were added into the cathodic reservoir, the charging plateau at a higher voltage and the discharging plateau at a lower voltage were greatly extended, which correspond to about 50% of $LiFePO_4$ (the specific capacity of $LiFePO_4$ is ~120 mA h g^{-1} based on a separate galvanostatic test in Swagelok cells) involved in the charging and discharging processes. The reaction yield of less than unity of $LiFePO_4$ might be due to the fact that some particles in the granules in the cathodic reservoir remained inaccessible by the iodide/iodine species while the electrolyte circulated through. It is believed that a better reservoir design, as well as a higher concentration of iodide (currently only 10 mM), will considerably improve the reaction yield of the active material. Assuming 50% porosity of the active material in the cathodic reservoir and considering 22.8 M of Li^+ storage in $LiFePO_4$, the gravimetric energy density and volumetric energy density of the cathodic tank of Li-I RFLB could reach ~370 W h kg^{-1} and

$\sim$670 W h L^{-1}, respectively, based on the active materials alone. In comparison, commercially available lithium-ion batteries have a gravimetric energy density of $>$200 W h kg^{-1} [18,19] and a vanadium redox flow battery has a tank energy density of $\sim$50 W h L^{-1}.[20] Hence the Li-I RFLB can achieve $>$10 times improvement in volumetric energy density compared to the most prevailing redox flow battery technology. Considering the capacity contributed from the redox species in the electrolyte (the concentration of LiI could be much higher), the energy density of the Li-I RFLB would be even higher.

The galvanostatic intermittent titration technique (GITT) measurements provide further information regarding the open-circuit voltage upon operation of the Li-I RFLB. As shown in Fig. 4b, the overpotential due to the IR drop across the membrane and electrolyte and the interfacial electron transfer on the cathode and anode could be isolated from the GITT measurements.[21] The open-circuit voltage recorded at various stages of charging and discharging is consistent with the potential of the redox molecule. The IR drop arising from the Li^+ transport across the membrane is largely responsible for the abrupt change of the GITT curve at each open circuit intermittency,[22] which is expected to be reduced if the Li^+ conductivity of the polymeric membrane is improved.

For 40 cycles, the Li-I RFLB cell shows $>$99% coulombic efficiency (CE) and $\sim$90% capacity retention (Fig. 4c). On average, each iodide molecule underwent 80 cycles of oxidation and reduction. The stability of the iodide species under different oxidation states and the robust nature of $LiFePO_4$ are mainly responsible for the excellent cycling performance. Fig. 4d shows a polarization curve presenting the discharge voltage and the corresponding power density with respect to the current densities at two different states of charge. The power density of the cell reaches the maximum 0.5 mW cm^{-2} at a current density of 0.3 mA cm^{-2} at the 100% state of charge. The relatively low power density is largely attributed to the resistance of the membrane and the low concentration of redox molecules. Since the solubility of LiI is $>$2 M in TEGDME, the power density is expected to be greatly enhanced when a higher concentration iodide is used in conjunction with a membrane that has high Li^+ conductivity.

We noticed that a lithium iodide redox flow battery, with lithium metal as the anode and 8 M LiI dissolved in an aqueous electrolyte as the liquid cathode, has recently been reported with good cycling stability.[23] However, the aqueous electrolyte presents a potential safety hazard—the reaction between the lithium metal and water would be disastrous in the case that the membrane separating the cathode and the anode fails. While using organic solvents in both the cathodic and the anodic half-cells will alleviate the problem, the solubility of LiI and consequently the energy density of the cell will be compromised. With the redox-targeting reactions between iodide and $LiFePO_4$, the Li-I RFLB elegantly resolves the above dilemma. The reachable energy density of the Li-I RFLB would be at least two-fold higher. Besides being a more effective design, the use of iodide to replace the previously reported ferrocene derivatives has several other advantages. Firstly, iodine is an inexpensive element and its reaction on carbon electrodes is sufficiently fast. Secondly, the use of a single redox molecule in the catholyte provides substantial benefits for both manufacturing and maintenance of the cell. Thirdly, the $I^-/I_3^-/I_2$ species are more immune to moisture or oxygen than the ferrocene derivatives, which is advantageous for a longer lifetime of the cells. Moreover, the interactions between iodide and $LiFePO_4$ also serve as an ideal model in the future design of redox molecules—the driving force for the redox-targeting reactions is large enough for fast kinetics while small enough for high energy efficiency.

In summary, lithium iodide coupled with $LiFePO_4$ was demonstrated to have high energy density and, to the extent of the measurements, excellent cyclic performance in the Li-I RFLB. Using a single redox molecule in the catholyte can lower the cost of manufacture and maintenance of the system. Li-I RFLBs can potentially achieve $>$10 times higher energy density than the conventional redox flow battery systems. Further improvement of the flow design and Li^+-conductivity across the membrane will make the Li-I RFLB a significant high-density energy storage solution for large-scale applications.

Acknowledgements

This research was supported by the National Research Foundation, Prime Minister's Office, Singapore, under its Competitive Research Program (CRP Award No. NRF-CRP8–2011–04).

Notes and references

1 J. Twidell and T. Weir, *Renewable energy resources*, Routledge, 2015.
2 G. Ren, G. Ma and N. Cong, *Renewable Sustainable Energy Rev.*, 2015, **41**, 225–236.
3 J. Y. Yong, V. K. Ramachandaramurthy, K. M. Tan and N. Mithulananthan, *Renewable Sustainable Energy Rev.*, 2015, **49**, 365–385.
4 R. Matthé and U. Eberle, The voltec system: Energy storage and electric propulsion, *In Lithium-Ion Batteries: Advances and Applications*, Elsevier, Amsterdam, The Netherlands, 2014, pp. 151–176.
5 S. Abada, G. Marlair, A. Lecocq, M. Petit, V. Sauvant-Moynot and F. Huet, *J. Power Sources*, 2016, **306**, 178–192.
6 Y. Zhao and H. R. Byon, *Adv. Energy Mater.*, 2013, **3**, 1630–1635.
7 X. Wei, W. Xu, M. Vijayakumar, L. Cosimbescu, T. Liu, V. Sprenkle and W. Wang, *Adv. Mater.*, 2014, **26**, 7649–7653.
8 Y. Zhao, Y. Ding, J. Song, G. Li, G. Dong, J. B. Goodenough and G. Yu, *Angew. Chem., Int. Ed.*, 2014, **53**, 11036–11040.
9 Y. Zhao, Y. Ding, J. Song, L. Peng, J. B. Goodenough and G. Yu, *Energy Environ. Sci.*, 2014, **7**, 1990–1995.
10 X. Wei, L. Cosimbescu, W. Xu, J. Z. Hu, M. Vijayakumar, J. Feng, M. Y. Hu, X. Deng, J. Xiao, J. Liu, V. Sprenkle and W. Wang, *Adv. Energy Mater.*, 2015, **5**, DOI: 10.1002/aenm.201400678.
11 Q. Huang, H. Li, M. Gratzel and Q. Wang, *Phys. Chem. Chem. Phys.*, 2013, **15**, 1793–1797.

12 F. Pan, J. Yang, Q. Huang, X. Wang, H. Huang and Q. Wang, *Adv. Energy Mater.*, 2014, **4**, DOI: 10.1002/aenm.201400567.
13 C. L. Bentley, A. M. Bond, A. F. Hollenkamp, P. J. Mahon and J. Zhang, *J. Phys. Chem. C*, 2015, **119**, 22392–22403.
14 C. Kuss, M. Carmant-Dérival, N. D. Trinh, G. Liang and S. B. Schougaard, *J. Phys. Chem. C*, 2014, **118**, 19524–19528.
15 J. R. Jennings, Q. Huang and Q. Wang, *J. Phys. Chem. C*, 2015, **119**, 17522–17528.
16 Q. Wang, S. M. Zakeeruddin, D. Wang, I. Exnar and M. Grätzel, *Angew. Chem., Int. Ed.*, 2006, **45**, 8197–8200.
17 A. S. Andersson, B. Kalska, L. Häggström and J. O. Thomas, *Solid State Ionics*, 2000, **130**, 41–52.
18 A. Masias, K. Snyder and T. Miller, in *Proceedings of the FISITA 2012 World Automotive Congress*, Springer Berlin Heidelberg, 2013, ch. 2, vol. 192, pp. 729–741.
19 P. Corporation, 2012.
20 J. Noack, N. Roznyatovskaya, T. Herr and P. Fischer, *Angew. Chem., Int. Ed.*, 2015, DOI: 10.1002/anie.201410823.
21 E. Ventosa, M. Skoumal, F. J. Vázquez, C. Flox and J. R. Morante, *J. Power Sources*, 2014, **271**, 556–560.
22 C. Jia, F. Pan, Y. G. Zhu, Q. Huang, L. Lu and Q. Wang, *Sci. Adv.*, 2015, **1**, DOI: 10.1126/sciadv.1500886.
23 Y. Zhao, L. Wang and H. R. Byon, *Nat. Commun.*, 2013, **4**, 1896.